Eur. Phys. J. Plus (2016) **131**: 208
DOI 10.1140/epjp/i2016-16208-2

THE EUROPEAN PHYSICAL JOURNAL PLUS

Regular Article

Renormalized entanglement in Heisenberg-Ising spin-1/2 chain with Dzyaloshinskii-Moriya interaction

Salman Khan[1,a] and Kalimullah Khan[2]

[1] Department of Physics, COMSATS Institute of Information Technology, Chak Shahzad, Islamabad, Pakistan
[2] Department of Physics, Quaid-i-Azam University, Islamabad, Pakistan

Received: 12 February 2016 / Revised: 28 April 2016
Published online: 22 June 2016 – © Società Italiana di Fisica / Springer-Verlag 2016

Abstract. The influence of the Dzyaloshinsky-Moriya (DM) interaction on entanglement in the one-dimensional spin-1/2 Heisenberg-Ising model is investigated via concurrence. The existence of two states, different in quantum properties and linked through a critical point by quantum phase transition, in the thermodynamic limit, are identified. The strong DM interaction delays quantum phase transition and hence shifts the boundary between the two phases to the region of the strong coupling constant. The increasing strength of the DM interaction strongly restores entanglement against its degradation arising from the increasing size of the system. The first derivative of the entanglement quantifier diverges to the critical point and is related directly to the divergence of the correlation length. The scaling behavior in the vicinity of the quantum critical point is also discussed.

1 Introduction

Entanglement [1] is one of the most fascinating and very perplexing phenomena of composite quantum systems. It has been extensively investigated under diverse conditions both for simple as well as many-body complicated systems [2–5]. Due to peculiarity in its nature and its key role in the foreseen quantum technology, it has been the pivot of theoretical research in different contexts for a very long time [6–8]. The studies of its dynamics in the context of relativity show that entanglement is a relative phenomenon and depends on the state of the observer [9–11]. In condensed matter physics, it is used as a detector for the existence of quantum phase transition (QPT), which occurs at absolute zero temperature [12]. Under different conditions, the studies of entanglement in various spin systems reveal its nonanalytic and scaling behaviors in the vicinity of the critical point [13–15].

The Ising and Heisenberg spin models are the few among the many-body systems, which have been the focus of different studies for long enough time due to the existence of their analytical solutions. Another class of interesting spin models, embodied with a variety of unusual behaviors specifically related to their ground states and thermal properties, are the Heisenberg-Ising spin systems. Such a model with alternating Heisenberg-Ising interactions were proposed and quantum mechanical solution for eigenfunctions were obtained by Lieb *et al.* [16]. The thermodynamical properties of such a model and its behavior under twisted boundary conditions were studied in [17,18]. Recently, the behavior of the model was examined under anisotropic Heisenberg exchange and DM interaction in two different studies [19, 20]. These studies reveal low-energy excitations with a gap and nonanalytic behavior of ground-state energy with a gapless excitation spectrum. One of the materials that can be modeled in terms of such competing interactions is the natural mineral azurite ($Cu_3(CO3)_2(OH)_2$), which exists in the so-called diamond-chain structure. Further details about different properties of such systems can be found in [21,22] and references therein.

Analytically studying the dynamics of the entanglement in many-body systems becomes very complex with the increasing dimensions of quantum systems. Special techniques are used to overcome such difficulties. One such technique is the well-known renormalization group (RG) technique. For several decades, the RG technique has been extensively used to explore the properties of many spin systems such as Monto Carlo RG [23,24] and density-matrix RG [25–29]. Recently, the approach of quantum renormalization group (QRG) is used to study the behavior of entanglement and QPT of anisotropic spin systems under different conditions [14,15]. It is found that with the considerable increasing number of iterations, the concurrence reaches two saturated values that represent two different phases of the spins

[a] e-mail: sksafi@comsats.edu.pk

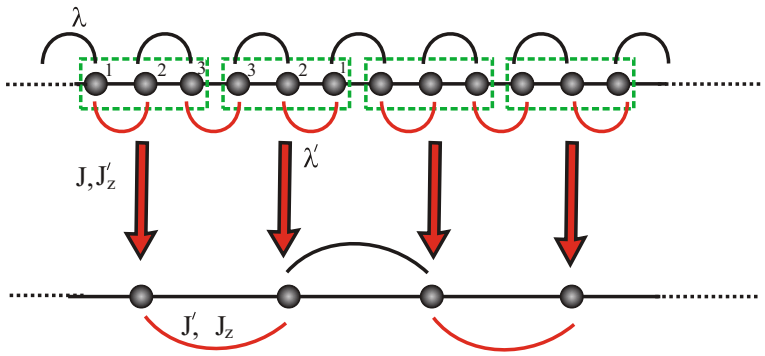

Fig. 1. Kadanoff's block renormalization group method of the Heisenberg-Ising spin-1/2 chain where each block consists of three sites.

system. These and some other studies [30,31] based on the approach of QRG show the existence of nonanalytical behaviors at quantum critical point. The studies of the effects of Dzyaloshinskii-Moriya (DM) interaction [32,33], which arises from the spin orbit interaction, in different spins models show remarkable behavioral changes in QPT and other related quantum critical phenomenon [34,35].

In this paper, we apply the QRG technique to study the behavior of the entanglement with the increasing size of the system via QRG iterations in the presence of DM interaction in the one-dimensional spin-1/2 Heisenberg-Ising model [16,36]. The Hamiltonian describing our system consists of four different parameters, three of them are coupling constants between the neighboring spins and one specifies the strength of the DM interaction. We first find relations that describe the behaviors of these parameters with increasing size of the system and then use them to thoroughly investigate the behavior of entanglement and QPT. We show that, although the effect of DM interaction on the dynamics of entanglement in our system is qualitatively parallel to its effects in the case of Ising and Heisenberg spin chains [37–39], it is considerably different quantitatively. In the thermodynamic limit, the behavior of the entanglement manifests two different phases of entangled and product states against the coupling parameter. These phases are separated by a critical point which is itself a function of the DM interaction. The nonanalytical behavior of the entanglement at the critical point and the scaling behavior near the critical point have also been analyzed.

This paper is organized as follows. In sect. 2, we apply the QRG method to investigate the model and renormalize the parameters for constructing the effective Hamiltonian of the system. In sect. 3, we investigate the behavior of the entanglement in the thermodynamic limit through a number of QRG iterations and discuss its nonanalytical and scaling behavior. In sect. 4, we summarize and conclude.

2 Quantum renormalization of the model

Since the focus of this work is to analyze the behavior of the entanglement in the Heisenberg-Ising model using the QRG technique, we therefore begin from a brief review of the basic concepts of the building blocks of this work. The QRG technique is a procedure which is used to eliminate system's degrees of freedom followed by an iteration. The concept behind the iterations is to reduce the number of variables step by step until a stable point is reached. To investigate the behavior of entanglement of our system through QRG technique, we use the approach of Kadanoff, where the lattice is divided into blocks, each comprising equal number of sites. This is an important approach for carrying analytical computation that can easily be extended to higher dimensions. In this set up, first the projection operators that act on the lower energy space of the system of each block are built. Then the projection of interblock interaction is mapped to an effective Hamiltonian which acts on the renormalized subspace [40–42]. To implement the procedure of this method, we first write the Hamiltonian of our spin model of $2N$ sites as follows [36]:

$$H = \sum_{i=1}^{N} \left[J\left(\sigma_{2i-1}^{x}\sigma_{2i}^{x}\right) + J\left(\sigma_{2i-1}^{y}\sigma_{2i}^{y}\right) + J_z\left(\sigma_{2i-1}^{z}\sigma_{2i}^{z}\right) + D(\sigma_{2i-1}^{x}\sigma_{2i}^{y} - \sigma_{2i-1}^{y}\sigma_{2i}^{x}) + \lambda(\sigma_{2i}^{z}\sigma_{2i+1}^{z})\right], \tag{1}$$

where $J > 0$, $J_z > 0$ and $\lambda \geqslant 0$ and characterize the coupling strengths between nearest spins on different sites. The parameter D represents the strength of DM interaction along the z-direction and $\sigma^{\alpha}(\alpha = x, y, z)$ are the Pauli matrices. The first three terms of the Hamiltonian correspond to the Heisenberg interaction, the fourth term represents the DM interaction and the last term represents the Ising interaction. As commented in the introduction, a number of materials can be approximately modeled with this type of Hamiltonian. So, it is important to look deeply into it through different perspectives. The Hamiltonian of eq. (1) is visualized in fig. 1, where the solid black curves represent the Ising interaction and the solid red curves represent the Heisenberg interaction. For clarity purposes, the positions

of spins in each block are labeled with numbers, such that its order reverses in each subsequent block. This helps to easily track the types of coupling between the adjacent blocks. Following the Kadanoff's approach, eq. (1) can be split into two parts as follows:

$$H = H^A + H^{AA}, \tag{2}$$

where $H^A = \sum_{L=1}^{2N/3} h_L^B$ represents the part contributed to the total Hamiltonian by the Hamiltonian h_L^B of a single block summed over the total number of blocks L in the system. For each block being composed of three spins, its explicit form for the L-th block can be written as

$$h_L^B = J\sigma_{1,L}^x\sigma_{2,L}^x + J\sigma_{1,L}^y\sigma_{2,L}^y + J_z\sigma_{1,L}^z\sigma_{2,L}^z + D(\sigma_{1,L}^x\sigma_{2,L}^y - \sigma_{1,L}^y\sigma_{2,L}^x) + \lambda\sigma_{2,L}^z\sigma_{3,L}^z. \tag{3}$$

Similarly, the H^{AA} in eq. (2) represents the part of the total Hamiltonian arising from the sum of the Hamiltonians of interaction between two nearest blocks. This can explicitly be written as

$$\begin{aligned} H^{AA} = \sum_{m=1}^{N/3} \big[& J\left(\sigma_{3,2m-1}^x\sigma_{3,2m}^x\right) + J\left(\sigma_{3,2m-1}^y\sigma_{3,2m}^y\right) + J_z\left(\sigma_{3,2m-1}^z\sigma_{3,2m}^z\right) \\ & + D(\sigma_{3,2m-1}^x\sigma_{3,2m}^y - \sigma_{3,2m-1}^y\sigma_{3,2m}^x) + \lambda(\sigma_{1,2m}^z\sigma_{1,2m+1}^z)\big]. \end{aligned} \tag{4}$$

The projectors for the subspace of a block can be constructed from its degenerate lowest energy eigenfunctions. It can be easily verified that the lowest eigenvalues of the L-th block Hamiltonian are doubly degenerate, whose corresponding degenerate eigenfunctions are given by

$$|\Psi_0\rangle = \frac{1}{\sqrt{1+|a|^2}}\left(ia|\uparrow\downarrow\uparrow\rangle + |\downarrow\uparrow\uparrow\rangle\right), \tag{5}$$

$$|\Psi_0'\rangle = \frac{1}{\sqrt{1+|b|^2}}\left(-ib|\uparrow\downarrow\downarrow\rangle + |\downarrow\uparrow\downarrow\rangle\right), \tag{6}$$

with

$$a = \left(\lambda + \sqrt{4D^2+4J^2+\lambda^2}\right)/2\,(D-iJ), \tag{7}$$

$$b = \left(\lambda - \sqrt{4D^2+4J^2+\lambda^2}\right)/2\,(D-iJ), \tag{8}$$

where $|\downarrow\rangle$ and $|\uparrow\rangle$ are the eigenfunctions of the Pauli spin operator σ^z. The corresponding degenerate eigenvalue is given by

$$E_0 = -J_z - \sqrt{\lambda^2+4J^2+4D^2}. \tag{9}$$

The original Hamiltonian is linked to the effective Hamiltonian through projector operator T_0, which is constructed in such a way that higher-energy terms are removed and the system stays in the lowest energy state. The relation between the effective Hamiltonian and the original Hamiltonian is given by

$$H^{eff} = T_0 H T_0^\dagger = T_0 H^A T_0^\dagger + T_0 H^{AA} T_0^\dagger, \tag{10}$$

where $T_0^\dagger$ is the Hermitian operator of T_0. The factorized form of the projector operator is given by

$$T_0 = \prod_{L=1}^{2N/3} T_0^L, \tag{11}$$

where T_0^L is the L-th block projector operator and is defined in terms of the lowest energy eigenfunctions in the following way:

$$T_0^L = |\Uparrow\rangle_L\langle\Psi_0| + |\Downarrow\rangle_L\langle\Psi_0'|. \tag{12}$$

In eq. (12), the kets $|\Uparrow\rangle_L$ and $|\Downarrow\rangle_L$ are the renamed states of the L-th block and can be thought of as a different spin-1/2 particle. Note that T_0^L is Hermitian and this can easily be checked. In order to write the effective Hamiltonian of the system in its final renormalized form, we first write the renormalized forms of the Pauli matrices as follows:

$$T_0\sigma_{i,L}^\alpha T_0^\dagger = \eta_i^\alpha\sigma_{i,L}^\alpha; \quad (i=1,3;\ \alpha=x,y,z), \tag{13}$$

where

$$\eta_3^x = \eta_3^y = \sqrt{\frac{4(D^2+J^2)}{4(D^2+J^2)+\lambda^2}}\,,$$
$$\eta_1^z = \frac{\lambda}{\sqrt{4(D^2+J^2)+\lambda^2}}\,,$$
$$\eta_3^z = 1. \tag{14}$$

Looking at fig. 1, one can immediately see that the Heisenberg interaction between the blocks occurs when spins with label 3 face each other and Ising interaction between the blocks takes place when spins with label 1 face each other. Due to this reason, we only have η_1^z in eq. (14). The effective renormalized Hamiltonian of the system can now be written, by using eqs. (13) and (14), in the following form:

$$H^{eff} = \sum_{m=1}^{N/3} \left[J'\left(\sigma_{2m-1}^x\sigma_{2m}^x\right) + J'\left(\sigma_{2m-1}^y\sigma_{2m}^y\right) + J_z'\left(\sigma_{2m-1}^z\sigma_{2m}^z\right) + D'\cdot(\sigma_{2m-1}^x\sigma_{2m}^y - \sigma_{2m-1}^y\sigma_{2m}^x) + \lambda'(\sigma_{2m}^z\sigma_{2m+1}^z)\right]. \tag{15}$$

The explicit forms of the renormalized parameters in eq. (15) in terms of the original one are given below

$$J' = \frac{4J(D^2+J^2)}{4(D^2+J^2)+\lambda^2}\,, \qquad J_z' = J_z,$$
$$D' = \frac{4D(D^2+J^2)}{4(D^2+J^2)+\lambda^2}\,, \qquad \lambda' = \frac{\lambda^3}{4(D^2+J^2)+\lambda^2}\,. \tag{16}$$

Equation (16) shows that J_z does not evolve as the size of the system increases. However, unlike the case of the Heisenberg spin model [38], the DM interaction D flows with the growing size of the system similar to the case of the Ising spin model [37]. From eq. (16) one can easily prove that

$$\chi' = \frac{1}{4(1+\kappa^2)}\chi^3, \tag{17}$$

with

$$\kappa = \frac{D}{J}\,, \qquad \chi = \frac{\lambda}{J}\,. \tag{18}$$

It is notable that a large system of $N = 3^{n+1}$ sites can be effectively described by a three-site block with the renormalized coupling constant after the n-th iteration of the QRG. The parameter κ and the parameter χ in eq. (18) can be considered as the rescaled values of DM interaction D and coupling constant λ in terms of coupling constant J.

A number of different measures for quantifying bipartite entanglement exist in the literature [43–47]. We, however, will use concurrence [2,3] to quantify entanglement between the spins of our system. For a bipartite state, it is given as

$$C = \max\{\eta_4 - \eta_3 - \eta_2 - \eta_1, 0\}, \tag{19}$$

where η_i $(i = 1,2,3,4)$ are the square roots of the eigenvalues in descending order of the matrix $R = \rho\widetilde{\rho}$, with $\widetilde{\rho} = (\sigma^y\otimes\sigma^y)\rho^*(\sigma^y\otimes\sigma^y)$. Here ρ^* represents the complex conjugate of the final density matrix ρ of a bipartite system. A system with $C = 1$ is maximally entangled and the one with $C = 0$ is separable.

3 Analysis of the renormalized entanglement

It takes less effort to analyze the ground-state entanglement of spin-1/2 Heisenberg-Ising chain through the QRG method in the presence of the DM interaction via the density matrix formalism. Keeping this in mind, we first construct the density matrix from the corresponding ground-state state function of the system. For the ground-state state function given in eq. (5), the density matrix becomes

$$\rho = |\Psi_0\rangle\langle\Psi_0|. \tag{20}$$

The state function $|\Psi_0\rangle$ represents the ground state of a block that consists of three spins and we are interested in the dynamics of only bipartite entanglement. To achieve our goal, the density matrix needs to be partial traced over

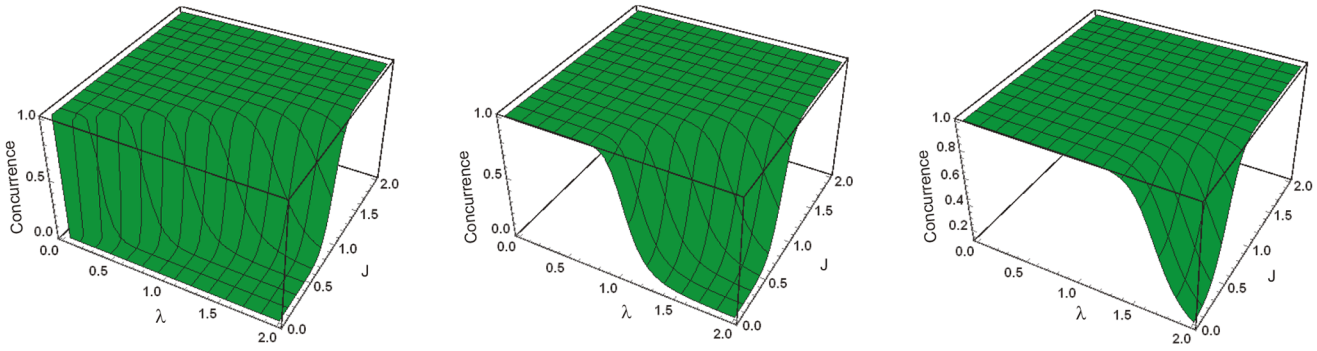

(a) (b) (c)

Fig. 2. The behavior of ground-state entanglement for three different choices of DM interaction D in thermodynamic limit against the coupling constants J and λ, is shown. The figures correspond to (a) $D = 0$, (b) $D = 0.5$, and (c) $D = 0.8$.

the dimensions of the subspace of one spin. A careful observation of the two state functions shows that partial tracing over the subspace of the spin with label 1 or at site with label 2 results in a product state whereas the same operation on the spin space at site with label 3 leaves the reduced bipartite state entangled. Therefore, to observe the behavior of bipartite entanglement in the system with DM interaction, we partial trace over the dimensions of the spin at site 3. The resulting reduced density matrix for the rest two spins of a block is as follows:

$$\rho_{12} = \frac{1}{1+|a|^2}\begin{bmatrix} 0 & 0 & 0 & 0 \\ 0 & |a|^2 & ia & 0 \\ 0 & -ia^* & 1 & 0 \\ 0 & 0 & 0 & 0 \end{bmatrix}. \tag{21}$$

It is now easy and straightforward to construct matrix R, as defined above, for calculating concurrence. One can then verify that all eigenvalues of R, except one, are zero. This makes the mathematical rigor easier for finding concurrence by using the definition given in eq. (19). The concurrence corresponding to ρ_{12} is then given by

$$C_{12} = 2\sqrt{\frac{D^2+J^2}{4(D^2+J^2)+\lambda^2}}. \tag{22}$$

From eq. (22), it can readily be seen that in the absence of DM interaction the result for concurrence of ref. [36] is retrieved. The presence of DM interaction and of the two coupling constants in the defining relation for C_{12} demonstrates that renormalization of these parameters strongly affect the behavior of bipartite entanglement between the nearest neighbors blocks of spins. For the ground state, the behavior of entanglement for three different values of the DM interaction ($D = 0, 0.5, 0.8$) in thermodynamic limit is shown in fig. 2. In the absence of the DM interaction (fig. 2(a)), the behavior of entanglement exhibits discontinuity along a line satisfying the condition $2J = \lambda$, which defines the quantum phase boundary of the model. At one side of the quantum phase boundary, the system is maximally entangled ($2J > \lambda$) and at the other side it is separable ($2J \leq \lambda$). The behavior of entanglement heavily depends on the strength of the DM interaction as shown in figs. 2(b) and (c). One can observe that the ranges of values of J and λ specifying the quantum phase boundary shrink with the increasing strength of the DM interaction. In other words, a considerably strong DM interaction may completely eliminate discontinuity from the dynamics of entanglement thereby leaving the system maximally entangled without demonstrating quantum phase transition. Apparently, this behavior of entanglement in the present system due to the presence of DM interaction is qualitatively identical to its behavior with DM interaction in the Ising and Heisenberg spin models [37–39]. However, quantitatively it is comparatively more sensitive to the DM interaction. This behavior may prove the spin systems, with different competing interactions between the nearest spins, more favorable for certain quantum information tasks whose realization solely depends on the existence of long-time entanglement.

In order to look more deeply into the behavior of entanglement in the presence of DM interaction with increasing size of the system degree of freedom via QRG iterations, we want to reduce the number of parameters and write eq. (22) with the help of eq. (17) into the following rescaled form:

$$C_{12} = 2\sqrt{\frac{\kappa^2+1}{4+4\kappa^2+\chi^2}}. \tag{23}$$

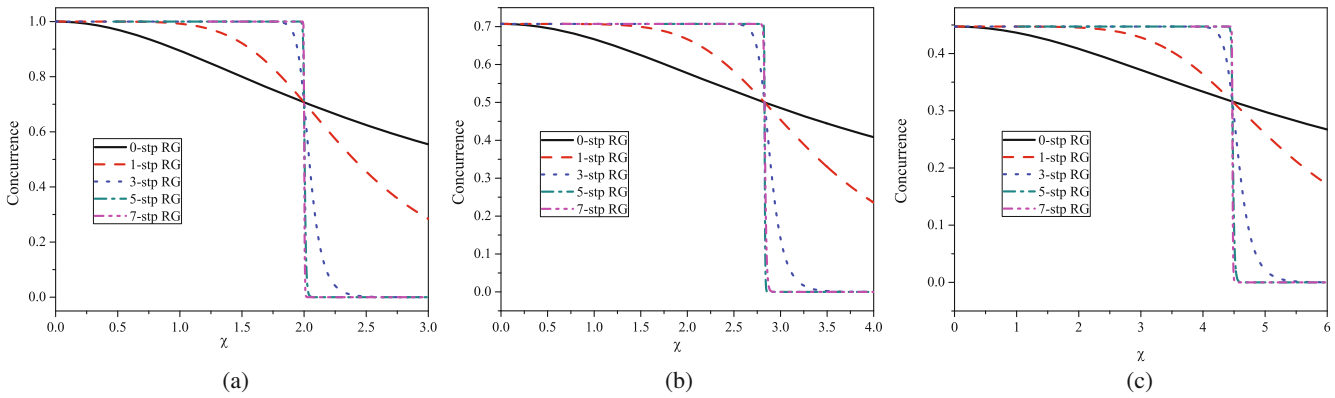

Fig. 3. Representation of the evolution of concurrence in terms of QRG iterations for three different values of the rescaled DM interaction parameter κ. The different behaviors of entanglement in the two different regions at large iterations of QRG correspond to the emerging phases of the system through phase transition (a) $\kappa = 0$, (b) $\kappa = 1$ and (c) $\kappa = 2$.

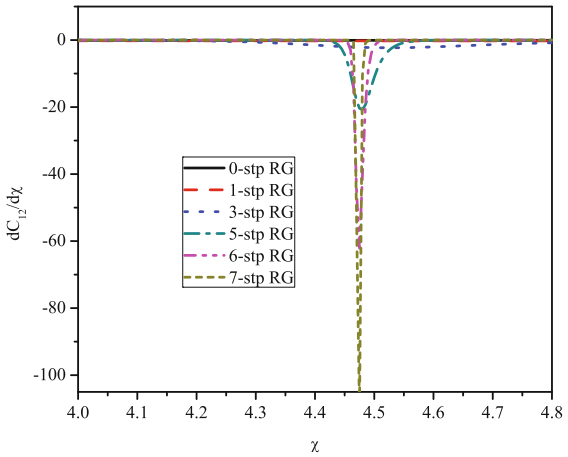

Fig. 4. The first derivative of the concurrence for $\kappa = 2$ and its manifestation toward divergence as the number of QRG iterations increases.

The effect of χ on the dynamics of entanglement with increasing size of the system is shown in fig. 3 for five different iterated values. It is easy to observe the drastic or nonanalytical change in the behavior of entanglement in thermodynamic limit obtained through high QRG iterations. For small size of the system (zero iteration), the entanglement instantly and gradually degrades as a continuous function of χ. However, as the number of iterations increases, two different regions, separated by a fixed value of χ, are developed in which the entanglement at either sides, relatively far from the fixed value of χ, remains frozen. The fixed value of χ at which all the curves meet, in fact, defines the critical point of the system and the two emerging regions represent two different phases of the system. The region to the left represents entangled phase of the system and the one to the right represents product state of the system. The critical point is not unique rather it depends on the value of κ, such that as κ increases it shifts to larger value of χ. Moreover, the increasing value of κ affects the entanglement for values of χ only to the left of the critical point in each of these figures. It is also notable that the initial degradation caused by the presence of κ is the same regardless of the size of the system.

The nonanalytic behavior of entanglement at the critical point in thermodynamic limit can further be explored through the divergence of its first derivatives. For the purpose of easiness, we will limit our further investigation to a single value of the rescaled DM interaction κ. The qualitative behavior of entanglement in the thermodynamic limit of the system for other choices of κ is identical.

The behavior of the first derivative of concurrence with respect to χ at different iterations for $\kappa = 2$ are plotted in fig. 4. The figure shows that each graph goes through a minimum at or in the vicinity of the critical point. The minimum becomes more prominent and shifts towards the critical point as the system touches the thermodynamic limit. The emerging singularity at the critical point is associated with the critical exponent of the system. To observe this link, we look into the minimum $\chi_{\min}$ of each curve and to their positions that how it scales with the increasing size of the system. This scaling behavior of the minimum of the first derivative of concurrence with the increasing size of the system is shown in fig. 5 for the choice of $\kappa = 2$. We observe that the minimum $\chi_{\min}$ is connected to the critical point through the entanglement exponent $\theta = 0.99$ as the size of the system grows through the relation $\chi_{\min} = \chi_c + N^{-\theta}$.

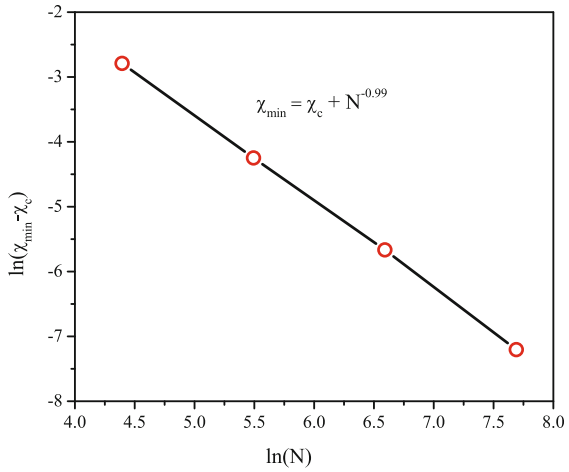

Fig. 5. The scaling behavior of $\chi_{\min}$ in terms of system size N for $\kappa = 2$, where $\chi_{\min}$ is the position of the minimum of each curve in fig. 4.

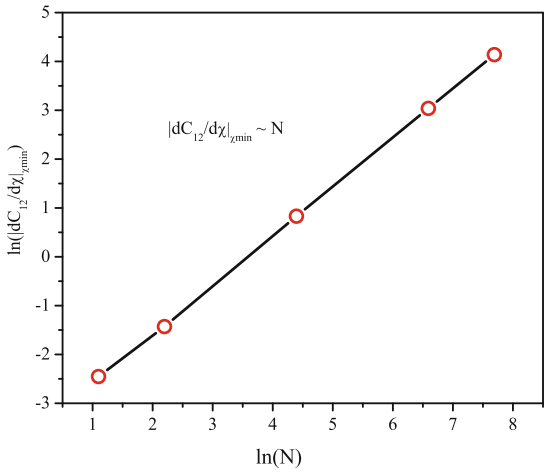

Fig. 6. The logarithm of the absolute value of minimum, $\ln(|\mathrm{d}C/\mathrm{d}\chi|_{\chi\min})$, *versus* the logarithm of chain size, $\ln(N)$, for $\kappa = 2$, which is linear and shows a scaling behavior. Each point corresponds to the minimum value of a single plot of fig. 4.

It has already been shown that the entanglement exponent θ itself is linked to the correlation length exponent ν close to the critical point through $\theta = 1/\nu$ [30,31]. Moreover, the scaling behavior of the first derivative of the concurrence at its minimum with the increasing size of the system has also been analyzed. Figure 6 shows the plot of $\ln(|\mathrm{d}C_{12}/\mathrm{d}\chi|_{\chi_{\min}})$ against $\ln(N)$ for $\kappa = 2$, which is linear and reflects that $|\mathrm{d}C_{12}/\mathrm{d}\chi|_{\chi_{\min}}$ goes almost like N. These results provide an adequate ground to believe that in the infinite Heisenberg-Ising spin-1/2 chain the QRG implementation of entanglement truly captures its critical behavior in the vicinity of the critical point.

4 Conclusions

In summary, we investigate the behavior of entanglement in the Heisenberg-Ising spin-1/2 chain in the presence of DM interaction through the QRG method using concurrence as entanglement quantifier. Our investigations show that entanglement is very sensitive to DM interaction and can be frozen to its initial value through strong DM interaction. In thermodynamic limit, the entanglement acquires two different behaviors thereby developing two regions one related to entangled and the other to separable states of the system. The two regions are linked through the critical point via quantum phase transition. The critical point is not unique, it rather depends on the strength of rescaled DM interaction κ in such a way that it shifts to large value of χ with increasing value of κ, and thereby enlarging the range of maintaining the phase of the entangled state of the system. In the thermodynamic limit, the divergent behavior of the first derivative of concurrence at the critical point in the presence of DM interaction becomes more pronounced. The scaling behavior of the entanglement in the vicinity of critical point, which characterizes how the critical point of the model is reached in the thermodynamic limit, is also studied. Its behavior leads us to obtain the critical exponent $\nu = 1/0.99 \approx 1$ in agreement with the universality class of the Ising model. The freezing of entanglement in thermodynamic limit through increasing DM interaction may prove Heisenberg-Ising spin systems useful for practical realization of quantum technology.

References

1. J.S. Bell, Physics **1**, 195 (1964).
2. X. Wang, Phys. Rev. A **66**, 044305 (2002).
3. X. Wang, Phys. Rev. A **66**, 034302 (2002).
4. L. Zhou, H.S. Song, Y.Q. Guo, C. Li, Phys. Rev. A **68**, 024301 (2003).
5. L. Amico, R. Fazio, A. Osterloh, V. Vedral, Rev. Mod. Phys. **80**, 517 (2008).
6. M.A. Nielsen I.L. Chuang, *Quantum Computation and Quantum Communication* (Cambridge University Press, Cambridge, 2000).
7. C.H. Bennet *et al.*, Phys. Rev. Lett. **70**, 1895 (1993).
8. C.H. Bennet, S.J. Wisener, Phys. Rev. Lett. **69**, 2881 (1992).
9. P.M. Alsing, David McMahon, G.J. Milburn, J. Opt. B: Quantum Semiclass. Opt. **6**, 834 (2004).
10. S. Khan, N.A. Khan M.K. Khan, Commun. Theor. Phys. **61**, 281 (2014).
11. S. Khan, Ann. Phys. **348**, 270 (2014).
12. S. Sachdev, *Quantum Phase Transitions* (Cambridge University Press, Cambridge, 2000).
13. T.J. Osborne, M.A. Nielsen, Phys. Rev. A **66**, 032110 (2002).
14. F.W. Ma, S.X. Liu, X.M. Kong, Phys. Rev. A **83**, 062309 (2011).
15. F.W. Ma, S.X. Liu, X.M. Kong, Phys. Rev. A **84**, 042302 (2011).
16. E. Lieb, T. Schultz, D. Mattis, Ann. Phys. (N.Y.) **16**, 407 (1961).
17. M. Gaudinf, Phys. Rev. Lett. **26**, 1301 (1971).
18. B.S. Shastry, B. Sutherland, Phys. Rev. Lett. **65**, 243 (1990).
19. H. Yao, J. Li, C.D. Gong, Solid State Commun. **121**, 687 (2002).
20. J. Strecka, L. Galisova, O. Derzhko, Acta Phys. Pol. A **118**, 742 (2010).
21. H. Kikuchi, Y. Fujii, M. Chiba, S. Mistsudo, T. Idehara, T. tonegawa, K. Okamoto, T. Sakai. T. Kuwai, H. Ohta, Phys. Rev. Lett. **94**, 227201 (2005).
22. N.S. Ananikian, L.N. Ananikyan, L.A. Chakhmakhchyan, O. Rojas, J. Phys.: Condens. Matter **24**, 256001 (2012).
23. S.K. Ma, Phys. Rev. Lett. **37**, 461 (1976).
24. P.J. Reynolds, H.E. Stanley, W. Klein, Phys. Rev. B **21**, 1223 (1980).
25. S.R. White, Phys. Rev. Lett. **69**, 2863 (1992).
26. S.R. White, Phys. Rev. B **48**, 10345 (1993).
27. T. Xiang, Phys. Rev. B **53**, 10445 (1996).
28. T. Nishino, J. Phys. Soc. Jpn. **64**, 3598 (1995).
29. S.R. White, D.J. Scalapino, Phys. Rev. Lett. **80**, 1272 (1998).
30. M. Kargarian, R. Jafari, A. Langari, Phys. Rev. A **76**, 060304(R) (2007).
31. M. Kargarian, R. Jafari, A. Langari, Phys. Rev. A **77**, 032346 (2008).
32. I. Dzyaloshinskii, J. Phys. Chem. Solids **4**, 241 (1958).
33. T. Moriya, Phys. Rev. **120**, 91 (1960).
34. J.H. Perk, H.W. Capel, Phys. Lett. A **58**, 115 (1976).
35. Z.N. Gurkan, O.K. Pashaev, *Two Qubit Entanglement in Magnetic Chains with DM Antisymmetric Anisotropic Exchange Interaction*, arXiv:0804.0710v2 [quanta-ph] (2008).
36. T.X. Dong, J.B. Qi, G. Wei, Chin. Phys. B **22**, 020308 (2013).
37. R. Jafari, M. Kargarian, A. Langari, M. Siahatgar, Phys. Rev. B **78**, 214414 (2008).
38. M. Kargarian, R. Jafari, A. Langari, Phys. Rev. A **79**, 042319 (2009).
39. M. Mahdian, M.B. Jeddi, M. Yahyavi M. Marahem, Int. J. Theor. Phys. **52**, 3830 (2013).
40. M.A. Martin-Delgado, G. Sierra, Int. J. Mod. Phys. A **11**, 3145 (1996).
41. A. Langari, Phys. Rev. B **69**, 100402(R) (2004).
42. A. Langari, Phys. Rev. B **58**, 14467 (1998).
43. Y.X. Chen, D. Yang, Quanta Inf. Proc. **1**, 389 (2003).
44. G. Vidal, R.F. Werner, Phys. Rev. A **65**, 032314 (2002).
45. E.M. Rains, Phys. Rev. A **60**, 179 (1999).
46. S. Hill, W.K. Wootters, Phys. Rev. Lett. **78**, 5022 (1997).
47. W.K. Wootters, Phys. Rev. Lett. **80**, 2245 (1998).